Science Signaling
AAAS

www.sciencesignaling.org/cgi/content/full/9/438/ra75/DC1

Supplementary Materials for

Binding of the cytoplasmic domain of CD28 to the plasma membrane inhibits Lck recruitment and signaling

Jessica Dobbins, Etienne Gagnon, Jernej Godec, Jason Pyrdol, Dario A. A. Vignali, Arlene H. Sharpe, Kai W. Wucherpfennig*

*Corresponding author. Email: kai_wucherpfennig@dfci.harvard.edu

Published 26 July 2016, *Sci. Signal.* **9**, ra75 (2016)
DOI: 10.1126/scisignal.aaf0626

This PDF file includes:

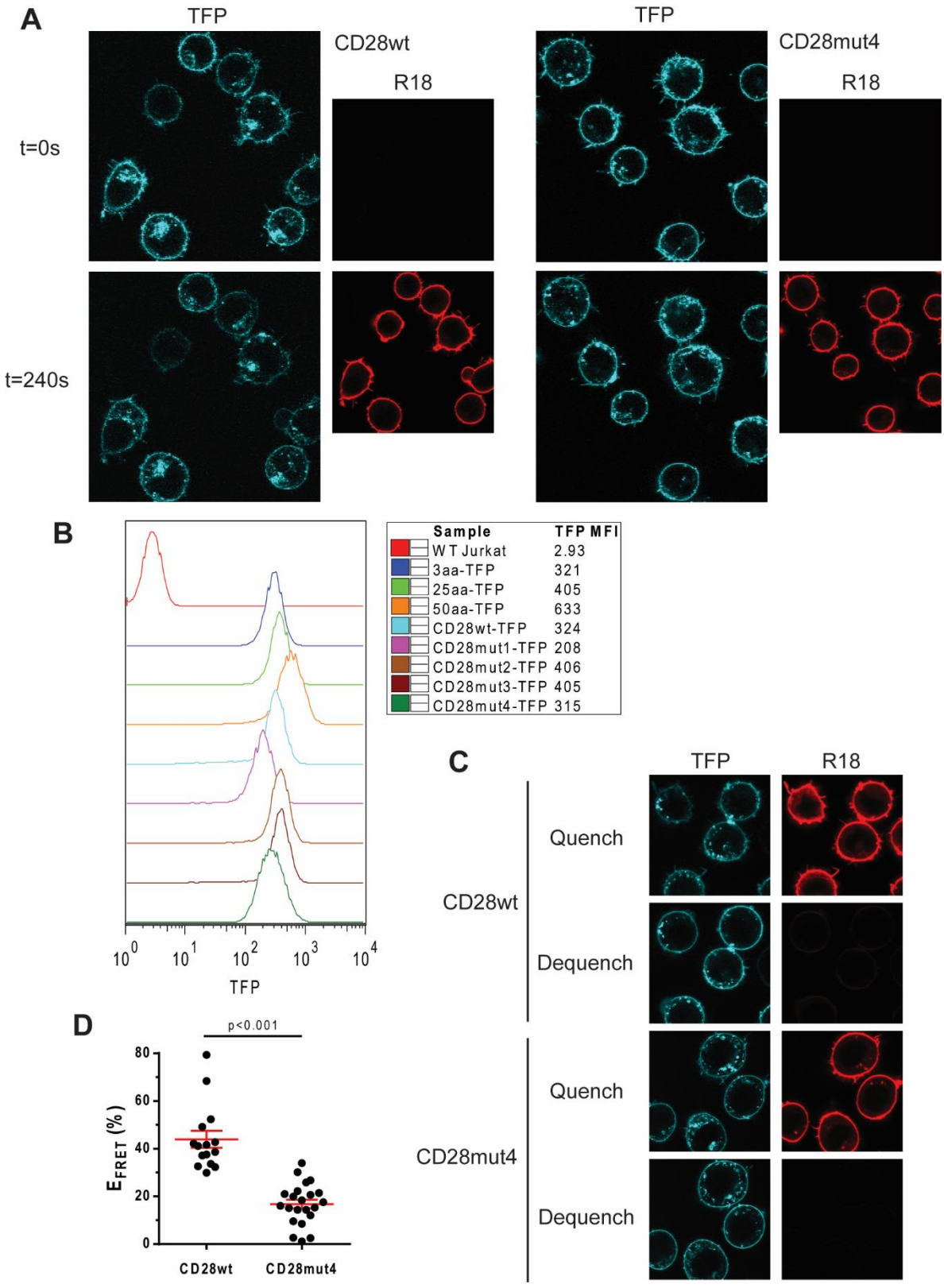

Fig. S1. Characterization of TFP-expressing cell lines and donor dequenching FRET measurements. (**A**) Jurkat cell transfectants expressing the indicated wild-type (WT) and mutant

CD28-TFP fusion proteins (FRET donor) were analyzed by confocal microscopy before (t = 0 s) and after (t = 240 s) labeling of the plasma membrane with octadecyl rhodamine B (R18) as a FRET acceptor. (**B**) Left: Overlaid histograms depict the flow cytometric analysis of TFP fluorescence for Jurkat single-cell clones expressing the indicated constructs. Right: TFP MFIs for each of the transfectants. (**C** and **D**) TFP donor dequenching FRET was analyzed by photobleaching of the R18 acceptor. Each point in (D) represents an individual cell. Mean E_{FRET} (%) and SEM values are also shown. The two groups were compared for statistically significant differences by two-tailed *t* test. Representative raw data are shown in (C). Images for both the TFP and R18 channels were captured before (quench) and after (dequench) selective photobleaching of R18. TFP fluorescence measured at the plasma membrane was used to calculate dequenching E_{FRET}.

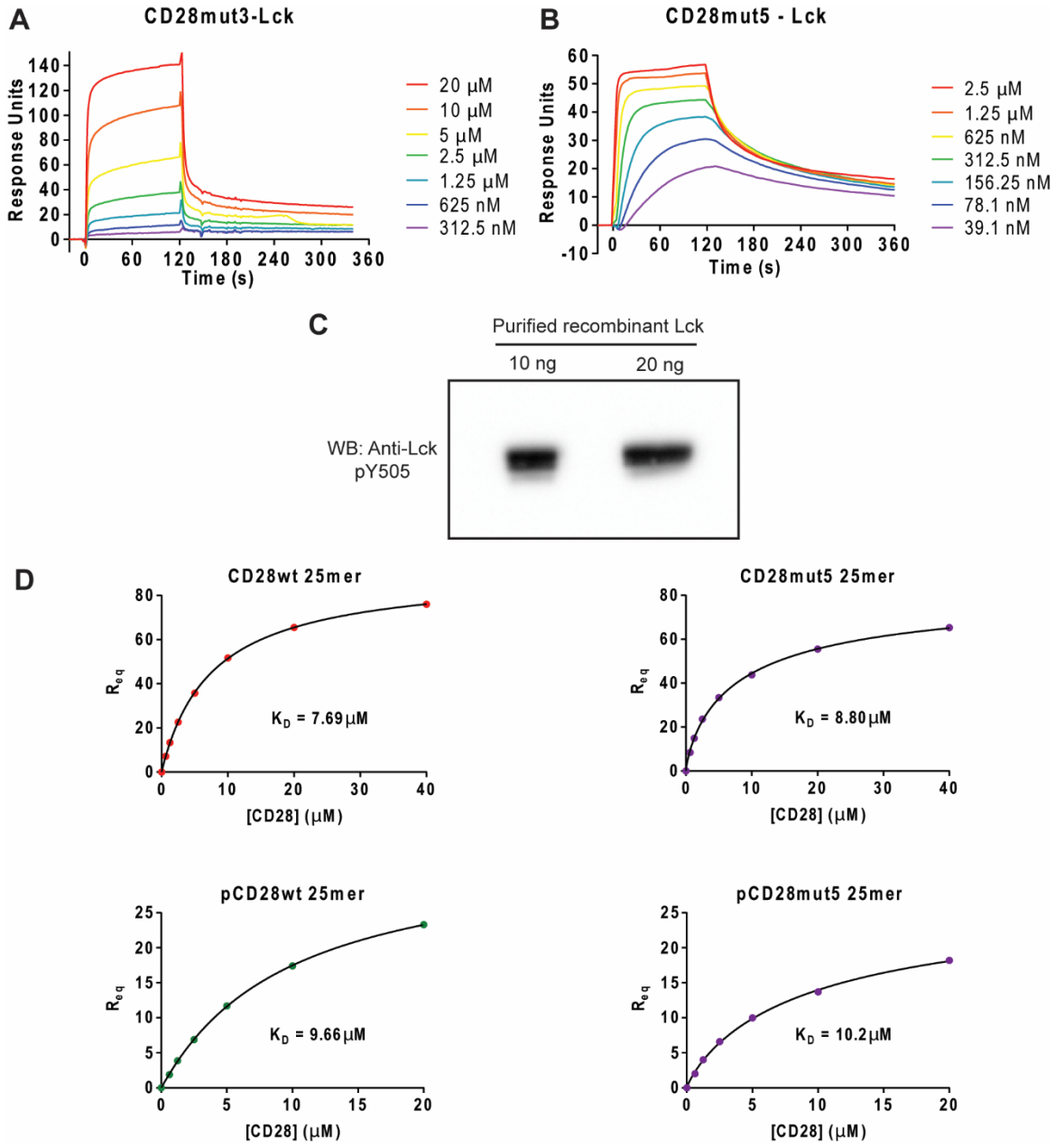

Fig. S2. SPR analysis of CD28-Lck binding. (**A** and **B**) The displayed curves depict SPR measurements of varying concentrations of CD28mut3 (A) or Mut5 (B) disulfide-linked dimers injected over a surface coated with Lck for 2-min association and 4-min dissociation periods. The bulk refractive index change was subtracted based on the signal from a surface with similar immobilized amounts of an irrelevant protein (HLA-DM). Data are representative of three experiments. (**C**) The indicated amounts of purified recombinant Lck, which was used for in vitro phosphorylation assays and SPR analysis throughout this study, were analyzed by Western blotting with an antibody specific to Lck phosphorylated at Tyr^{505}. Data are representative of two experiments. (**D**) Equilibrium binding analysis was performed for the binding of the indicated 25-mer, disulfide-linked CD28 dimers to immobilized full-length Lck after bulk refractive index subtraction based on a flow cell coated with HLA-DM (as a negative control protein). Plots of R_{eq} at the indicated concentrations of CD28 are shown. Data are representative of two experiments. Peptides represented the 25 C-terminal amino acid residues of $CD28_{CD}$ (residues 194 to 218) with or without phosphorylation at Tyr^{207}. Binding studies were performed in the absence of ATP to prevent phosphorylation of $CD28_{CD}$ by Lck. K_D was calculated by fitting to a saturation binding model with Hill slope.

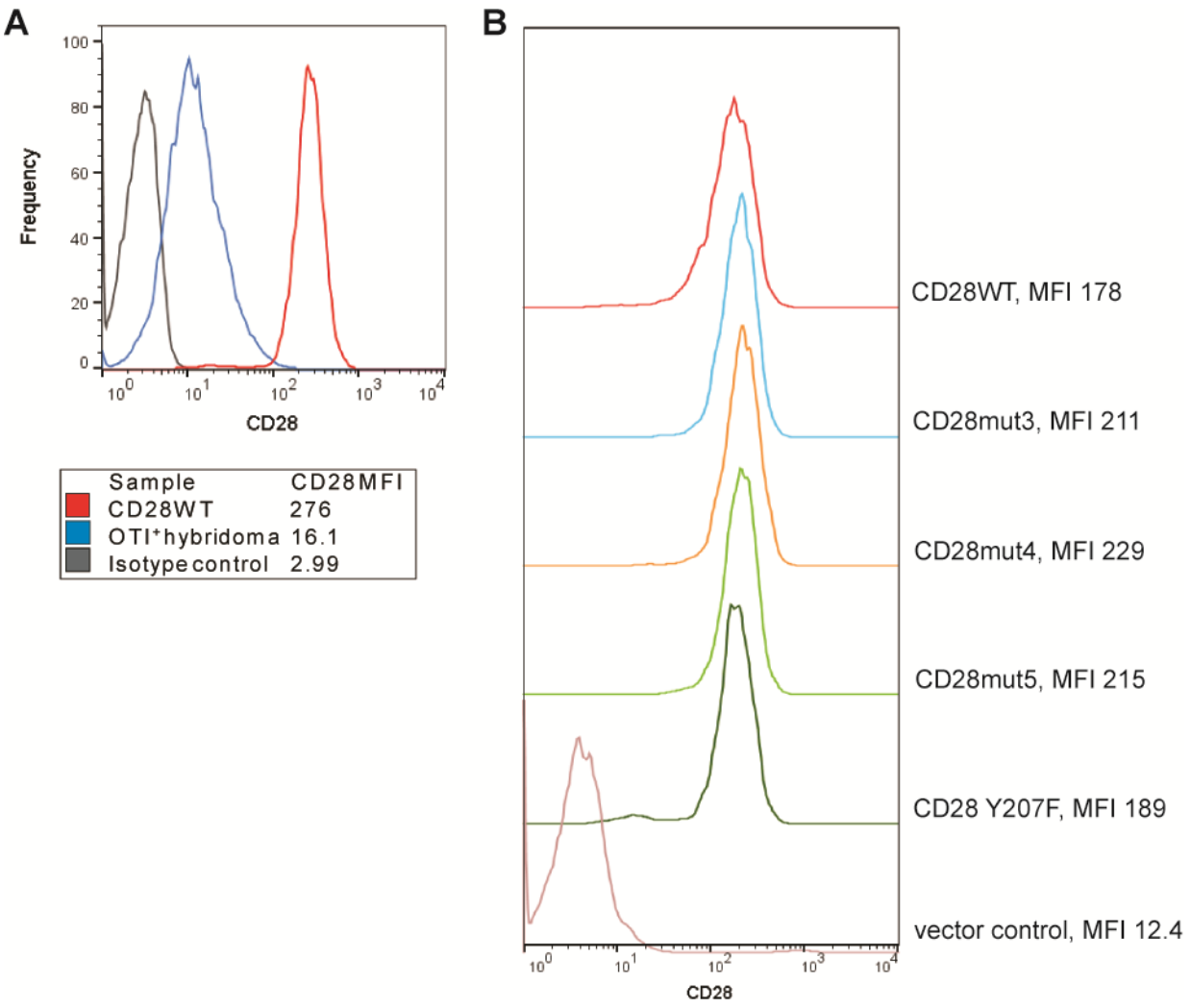

Fig. S3 Analysis of the cell surface abundance of CD28 in OT-I$^+$ hybridomas. (**A**) The cell surface abundance of CD28 in OT-I$^+$ hybridoma cells that were or were not transduced with a retrovirus encoding a CD28WT expression construct was determined by flow cytometric analysis. (**B**) OT-I$^+$ hybridoma cells transduced with retroviruses expressing CD28WT, the indicated mutant CD28 constructs, or a negative control were analyzed by flow cytometry, sorted based on ZsGreen amount, and then sorted for matched CD28 cell surface abundance.

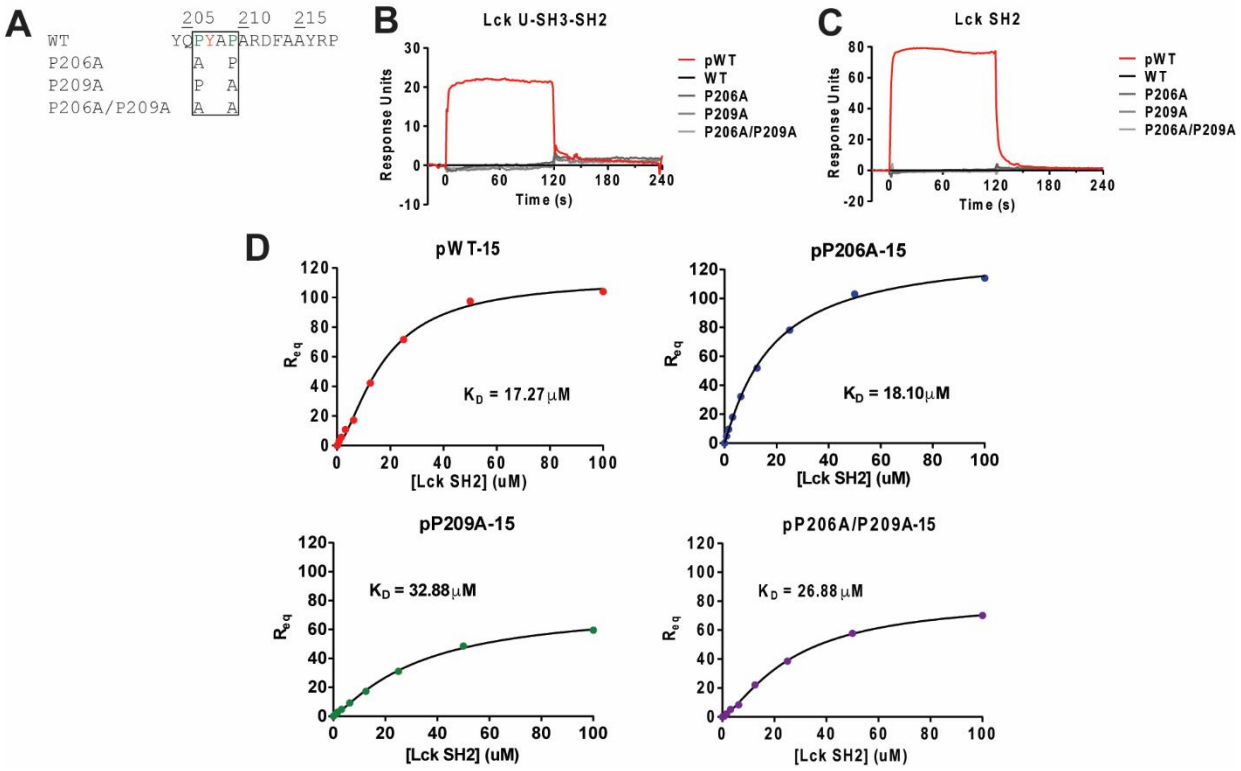

Fig. S4. SPR analysis of the interaction between the CD28 15-mer peptide and Lck SH2 or Lck U-SH3-SH2. (**A**) A panel of peptides was prepared representing the C-terminal 15 amino acid residues of $CD28_{CD}$ (residues 204 to 218). The contribution of the P206A and P209A mutations was examined individually and in combination, and each peptide was prepared in both phosphorylated (on Tyr^{207}, indicated by the prefix "p") and nonphosphorylated forms. (**B** and **C**) The indicated peptides were coated to approximately the same density on a streptavidin surface and the Lck U-SH3-SH2 domain construct (B) or the Lck SH2 domain (C) was injected at a concentration of 5 μM over each of the surfaces after subtraction of the bulk refractive index change based on a streptavidin surface. (**D**) The purified Lck SH2 domain was injected at varying concentrations over surfaces coated with the indicated peptides. R_{eq} was plotted versus the Lck SH2 domain concentration. K_D was calculated by fitting to a saturation binding model with a Hill slope.

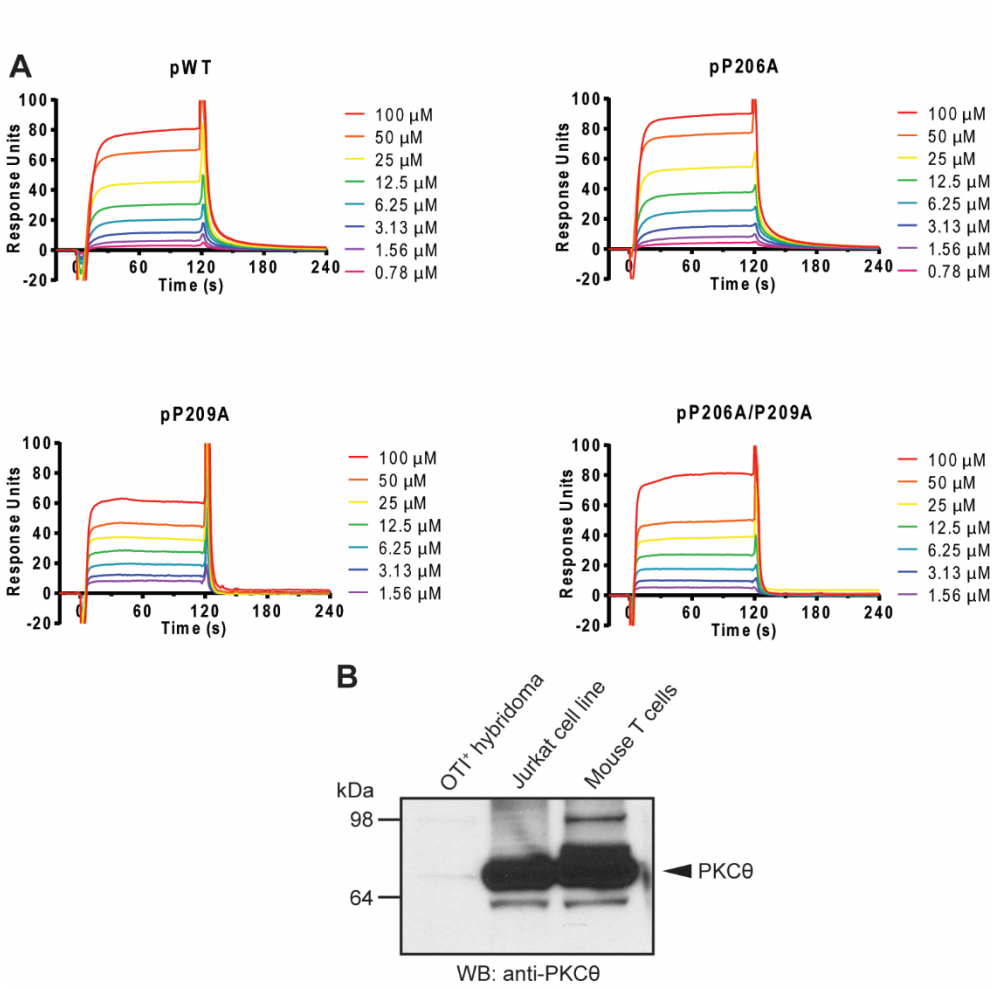

Fig. S5. Equilibrium binding measurements of the interaction between the Lck SH2 domain and the CD28 PYAP motif. (**A**) The indicated peptides (sequences shown in fig. S4A) were coated to approximately the same density on a streptavidin surface. The displayed curves depict SPR measurements resulting from injection of the indicated concentrations of purified Lck SH2 domain. The bulk refractive index change was subtracted based on a control surface coated with nonphosphorylated CD28 WT 15-mer peptide, which exhibited no binding to the Lck SH2 domain. Similar results were obtained by subtracting signal from a streptavidin surface. Data are representative of three experiments. (**B**) PKCθ abundance was compared between OT-I$^+$ hybridoma (mouse), Jurkat (human), and primary mouse T cells (1×10^5 cells per lane) by Western blotting analysis with an anti-PKCθ antibody. The Western blot was overexposed so that the bands in the lanes containing the OT-I$^+$ hybridoma cells were detectable.

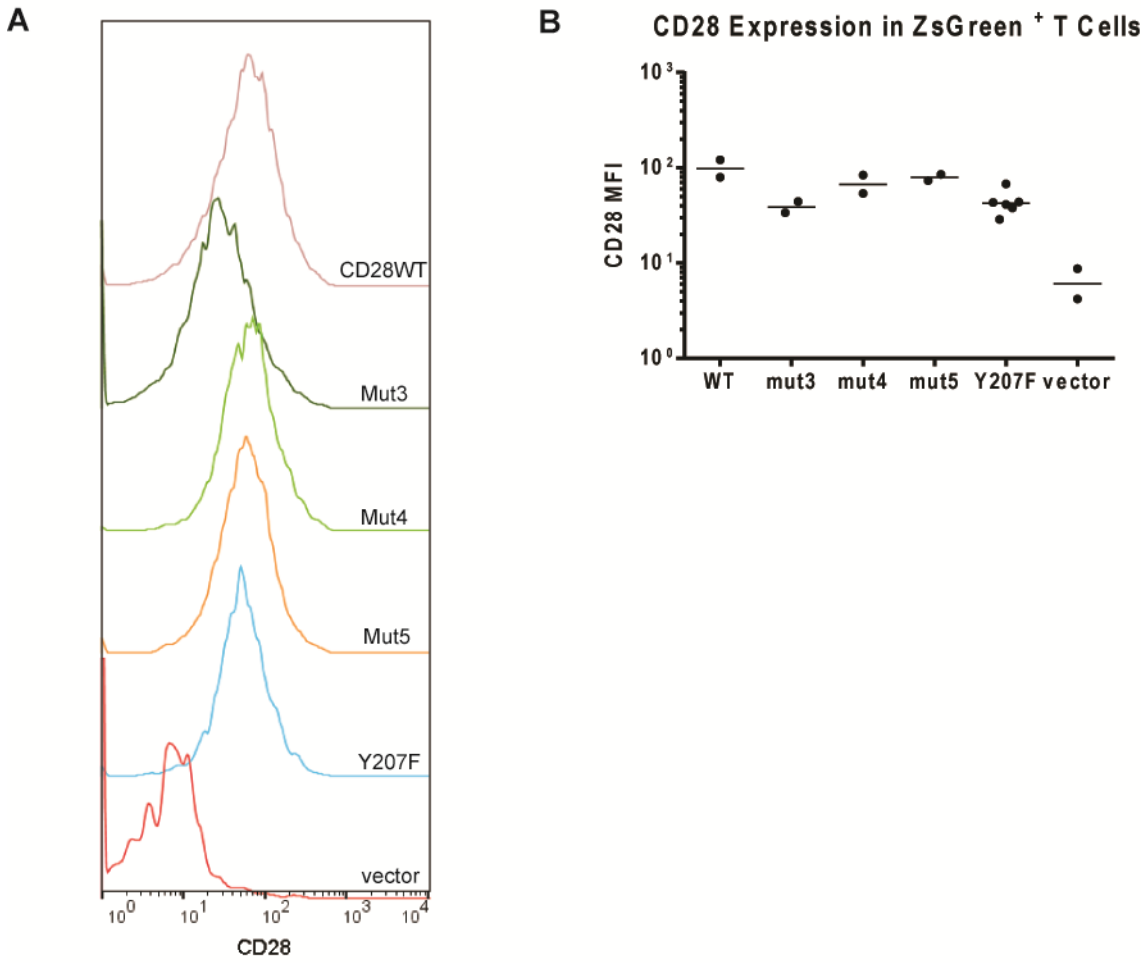

Fig. S6. Flow cytometric analysis of splenic T cells from transduced bone marrow chimeric mice. (**A**) Flow cytometric analysis of the cell surface abundance of CD28 for ZsGreen^{+} splenic T cells from recipients of bone marrow cells transduced with retroviruses expressing the indicated CD28 constructs or empty vector. (**B**) CD28 MFIs from the experiments shown in (A) were determined. Data are geometric means for multiple samples. Each symbol represents an individual mouse.

Table S1. Identification of the tyrosine residues of $CD28_{CD}$ that are phosphorylated by Lck. CD28WT and Mut5 dimer peptides were normalized for input by OD_{280nm} before being subjected to an in vitro phosphorylation reaction with recombinant Lck. Reaction products were resolved by SDS-PAGE, and the region of the gel corresponding to the CD28 dimer was excised. Gel slices were submitted to the Taplin Mass Spectrometry Facility (Harvard Medical School) for analysis of phosphotyrosine modification. Peptides were fragmented by in-gel tryptic digest and the resulting peptide mixtures were analyzed by LC/MS-MS. The table depicts the relative phosphorylation of each tyrosine based on the peak area of the phosphorylated fragment compared to the total peak area for that fragment (sum of phosphorylated and unmodified).

Phosphorylation Site	CD28wt	CD28mut5
Y189 (YMNM)	20.2%	32.8%
Y204	Not detected	2.1%
Y207 (PYAP)	20.9%	35.7%
Y215	2.9%	10.0%